

## Notes

## Molecular Structure and Magnetic Properties of Acetato-Bridged Lanthanide(III) Dimers

Athanassios Panagiotopoulos,<sup>†</sup>  
 Theodoros F. Zafiropoulos,<sup>†</sup> Spyros P. Perlepes,<sup>\*,†</sup>  
 Evangelos Bakalbassis,<sup>‡</sup> Isabelle Masson-Ramade,<sup>§</sup>  
 Olivier Kahn,<sup>\*,§</sup> Aris Terzis,<sup>||</sup> and  
 Catherine P. Raptopoulou<sup>||</sup>

Department of Chemistry, University of Patras,  
 26500 Patra, Greece, Laboratory of Applied Quantum  
 Chemistry, Department of General and Inorganic Chemistry,  
 Faculty of Chemistry, Aristotle University of Thessaloniki,  
 P.O. Box 135, 54006 Thessaloniki, Greece,  
 Laboratoire de Chimie Inorganique, URA CNRS No. 420,  
 Université de Paris Sud, 91405 Orsay, France, and  
 Institute of Material Science, NRCPS Demokritos,  
 15310 Aghia Paraskevi Attikis, Greece

Received March 10, 1995

Structural, magnetic, and EPR studies of diaquatetrakis( $\mu$ -acetato)dycopper(II) have provided important insight into the magnetic interaction phenomenon in polynuclear species involving 3d ions.<sup>1–3</sup> This compound may be considered as the archetype of the exchange-coupled copper(II) dimers. Until now, no compound of the same nature involving lanthanide(III) ions had been reported, and the factors determining the sign and the magnitude of the magnetic interaction between lanthanide(III) ions are far from being well understood.<sup>4,5</sup> Herein we report on the synthesis, the structure and the magnetic properties of two lanthanide(III) dimers, namely  $[\text{Ln}_2(\text{CH}_3\text{CO}_2)_6(\text{phen})_2]$  with phen = *o*-phenanthroline and Ln = Ce (1) and Gd (2).

The molecular structure of 1 is shown in Figure 1. The molecular unit is dimeric with an inversion center. The Ce(III) ions are linked by four acetato groups. Two of them bridge in the classical  $\eta^1:\eta^1:\mu_2$  fashion, and the other two bridge in the less common  $\eta^2:\eta^1:\mu_2$  fashion; these latter have an oxygen atom (O(2), O(2\*)) bound terminally to one cerium atom, and the other oxygen atom (O(1), O(1\*)) bound in a  $\mu_2$ -bridging manner to both cerium atoms, forming a monoatomic bridge. One terminal phen molecule and one bidentate chelating acetato group complete a nine-coordination at each metal. Due to the inversion center, the CeO(1)Ce\*O(1\*) network is perfectly planar. The  $[\text{Ln}_2(\eta^1:\eta^1:\mu_2\text{-RCO}_2)_2(\eta^2:\eta^1:\mu_2\text{-RCO}_2)_2]$  network is

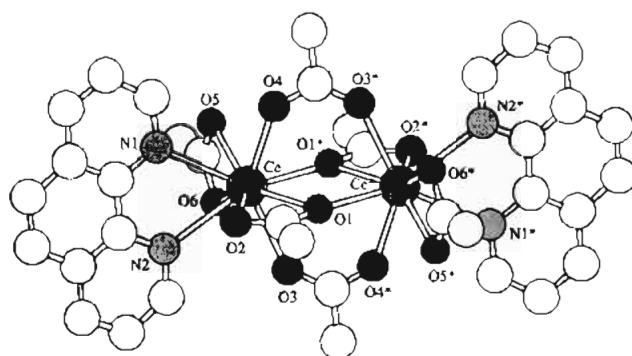


Figure 1. Molecular structure of 1. Selected bond lengths (Å) are as follows: Ce–O(1) = 2.726(3), Ce–O(1\*) = 2.441(4), Ce–O(2) = 2.552(3), Ce–O(3) = 2.433(3), Ce–O(4) = 2.419(3), Ce–O(5) = 2.588(4), Ce–O(6) = 2.546(4), Ce–N(1) = 2.681(3), and Ce–N(2) = 2.677(4). Selected bond angles (deg) are as follows: O(1)–Ce–O(1\*) = 77.5(1), O(1)–Ce–O(2) = 48.8(1), and Ce–O(1)–Ce\* = 102.5(1). The Ce–Ce separation is equal to 4.035(3) Å. Unstarred and starred atoms are related by the inversion center.

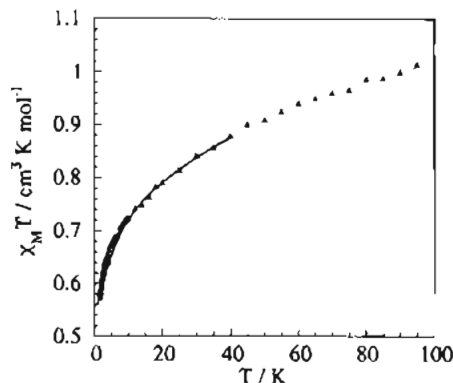


Figure 2.  $\chi_M T$  vs  $T$  curves for 1: ( $\blacktriangle$ ) experimental data; (—) calculated curve below 30 K.

unique for Ce(III) and rare for other lanthanide(III) ions,<sup>6</sup> the majority of known lanthanide(III) species which display the same arrangement of four bridging carboxylato groups are polymers.<sup>6,7</sup>

The coordination sphere of the cerium atom is best described as a distorted monocapped square antiprism with O(1) as the capping atom and atoms O(1\*), O(3), O(2), O(4) and N(1), N(2), O(6), O(5) as the capped and noncapped faces, respectively.

Both molar magnetic susceptibilities,  $\chi_M$ , and EPR spectra for 1 and 2 have been measured. The  $\chi_M T$  vs  $T$  plot for 1 continuously decreases as the temperature  $T$  is lowered, and reaches  $0.57 \text{ cm}^3 \text{ K mol}^{-1}$  at 1.7 K (see Figure 2). In the absence of interaction, the  $^2F_{5/2}$  free-ion ground state of Ce(III) is split into three Kramers doublets by the ligand field, and  $\chi_M T$  is expected to reach a plateau in the low-temperature range where only the ground Kramers doublet is thermally populated. The continuous decrease of  $\chi_M T$  as  $T$  approaches absolute zero indicates that the two local Kramers doublets interact to give a nonmagnetic (at the first order) ground state and a pseudotriplet

<sup>†</sup> University of Patras.

<sup>‡</sup> Aristotle University of Thessaloniki.

<sup>§</sup> Université de Paris-Sud.

<sup>||</sup> NRCPS Demokritos.

- (1) Bleaney, B.; Bowers, K. D. *Proc. R. Soc. London, A* **1952**, *214*, 451.
- (2) Martin, R. L. In *New Pathways in Inorganic Chemistry*; Ebsworth, E. A. V., Maddock, A., Sharpe, A. G., Eds.; Cambridge University Press: London, 1968.
- (3) Kahn, O. *Molecular Magnetism*; VCH: New York, 1993.
- (4) Füller, A.; Güdel, H. U.; Krausz, E. R.; Blank, H. *Phys. Rev. Lett.* **1989**, *64*, 68.
- (5) Lueken, H.; Hannibal, P.; Handrick, K. *Chem. Phys.* **1990**, *143*, 151.

- (6) (a) Smith, P. H.; Ryan, R. R. *Acta Crystallogr., Sect. C* **1992**, *48*, 2127, and references therein. (b) Ouchi, A.; Suzuki, Y.; Ohki, Y.; Koizumi, Y. *Coord. Chem. Rev.* **1988**, *92*, 29. (c) Lossin, A.; Meyer, G.; Fuchs, R.; Strähle, J. Z. *Naturforsch.* **1992**, *47*, 179.
- (7) Csöregi, I.; Huskowska, E.; Legendziewicz, J. *Acta Crystallogr., Sect. C* **1992**, *48*, 1030 and references therein.

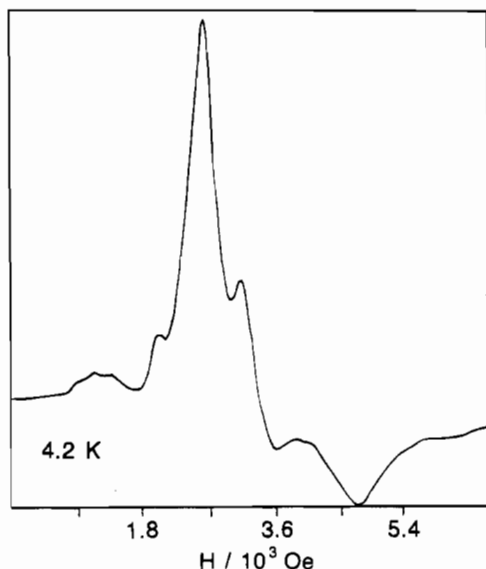


Figure 3. X-band powder EPR spectrum at 4.2 K for 1.

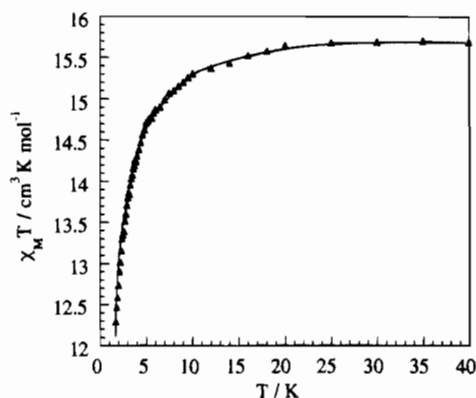


Figure 4.  $\chi_M T$  vs  $T$  curves for 2: ( $\blacktriangle$ ) experimental data; (—) calculated curve.

excited state. The  $\chi_M T$  vs  $T$  data below ca. 20 K may be well interpreted with the equation

$$\chi_M = \frac{2N\beta^2 g^2}{kT[3 + \exp(-J/kT)]} + \text{TIP} \quad (1)$$

where  $J = -0.75 \text{ cm}^{-1}$  is the energy gap between those two states, and  $\text{TIP} = 660 \times 10^{-6} \text{ cm}^3 \text{ mol}^{-1}$  is a temperature independent paramagnetism. This TIP contribution accounts for the coupling between ground and excited local Kramers doublets arising from the  $^2F_{5/2}$  free-ion state through the Zeeman perturbation. The X-band powder EPR spectrum for 1 agrees with such a view. This spectrum at 4.2 K, shown in Figure 3, looks like the spectrum of a triplet state with an axial zero-field splitting parameter,  $|D| = 0.21 \text{ cm}^{-1}$ , smaller than the incident quantum.<sup>8</sup> The spectrum vanishes above ca. 12 K.

The situation is much simpler for 2. The  $\chi_M T$  vs  $T$  curve is shown in Figure 4.  $\chi_M T$  is constant and equal to  $15.80(6) \text{ cm}^3 \text{ K mol}^{-1}$  down to ca. 25 K, and then decreases more and more rapidly as  $T$  is lowered further. These magnetic susceptibility data very closely follow the equation deduced from the isotropic

Table 1. Crystallographic Data for Compound  $[\text{Ce}_2(\text{CH}_3\text{CO}_2)_6(\text{phen})_2]$  (1)

chem formula	$\text{C}_{36}\text{H}_{34}\text{N}_4\text{O}_{12}\text{Ce}_2$	fw	994.84
$a$ (Å)	9.883(1)	space group	$P\bar{1}$
$b$ (Å)	9.875(1)	$T$ (°C)	23
$c$ (Å)	10.119(1)	$\lambda(\text{Mo K}\alpha)$ (Å)	0.7107
$\alpha$ (deg)	99.96(1)	$\mu$ ( $\text{cm}^{-1}$ )	23.5
$\beta$ (deg)	108.69(1)	$\rho_{\text{calc}}$ ( $\text{g cm}^{-3}$ )	1.80
$\gamma$ (deg)	89.91(1)	$R^a$	0.0276
$V$ (Å <sup>3</sup> )	920.0(1)	$R_w^b$	0.0320
$Z$	1		

$$^a R = \sum(|F_o| - |F_c|)/\sum|F_o|. \quad ^b R_w = [\sum w(|F_o| - |F_c|)^2/\sum(|F_o|)^2]^{1/2}.$$

Table 2. Positional ( $\times 10^4$ ) and Equivalent Isotropic Thermal Parameters (Å<sup>2</sup>  $\times 10^4$ ) for the Non-Hydrogen Atoms of  $[\text{Ce}_2(\text{CH}_3\text{CO}_2)_6(\text{phen})_2]$  (1) with Esd's in Parentheses

atom	$x$	$y$	$z$	$U_{\text{eq}}^a$
Ce	-1252.1(3)	1469.1(2)	526.8(3)	324
O(1)	901(4)	-164(3)	1607(3)	462
O(2)	138(4)	1266(4)	3082(3)	499
O(3)	-2263(4)	-835(3)	311(4)	537
O(4)	973(4)	2439(3)	478(4)	529
O(5)	-2304(4)	3159(4)	-1183(4)	591
O(6)	-3798(4)	1618(4)	-1096(4)	588
C(1)	953(5)	350(4)	2866(5)	381
C(2)	1998(7)	-140(7)	4069(6)	563
C(3)	-2061(5)	-2058(5)	-130(5)	433
C(4)	-3161(7)	-3146(6)	-258(11)	704
C(5)	-3561(5)	2664(5)	-1567(5)	424
C(6)	-4598(8)	3237(8)	-2408(7)	805
N(1)	-1066(4)	4001(4)	2068(4)	378
N(2)	-2941(4)	2008(4)	2138(4)	379
C(7)	-219(5)	4990(5)	1968(5)	454
C(8)	-3(6)	6314(5)	2836(6)	497
C(9)	-675(5)	6566(5)	3822(6)	446
C(10)	-1577(5)	5551(4)	3958(5)	375
C(11)	-2293(5)	5738(5)	4998(5)	462
C(12)	-3184(6)	4752(5)	5059(6)	512
C(13)	-3474(5)	3463(5)	4075(5)	412
C(14)	-4460(6)	2446(6)	4051(6)	543
C(15)	-4677(6)	1244(6)	3064(6)	532
C(16)	-3890(5)	1075(5)	2161(6)	468
C(17)	-2742(4)	3220(4)	3085(4)	326
C(18)	-1769(5)	4267(4)	3015(5)	336

<sup>a</sup>  $U_{\text{eq}}$  is defined as one-third of the trace of the orthogonalized  $U_{ij}$  tensor. The exponential factor for  $U_{ij}$  has the form  $2\pi^2(U_{11}h^2a^{*2} + U_{22}k^2b^{*2} + 2U_{12}hka^*b^* + 2U_{13}hla^*c^* + 2U_{23}klb^*c^*)$ .

spin Hamiltonian  $H = -JS_{\text{Gd1}} \cdot S_{\text{Gd2}}$  with the quantum numbers  $S_{\text{Gd1}} = S_{\text{Gd2}} = 7/2$ . This equation is

$$\chi_M = \left( \frac{2N\beta^2 g^2}{kT} \right) \times \left( \frac{e^x + 5e^{3x} + 14e^{6x} + 30e^{10x} + 55e^{15x} + 91e^{21x} + 140e^{28x}}{1 + 3e^x + 5e^{3x} + 7e^{6x} + 9e^{10x} + 11e^{15x} + 13e^{21x} + 15e^{28x}} \right) \quad (2)$$

with

$$x = J/kT \quad (3)$$

The isotropic interaction parameter  $J$  is found to be equal to  $-0.053 \text{ cm}^{-1}$ , and the Zeeman factor  $g$ , assumed to be isotropic, to be equal to 2.0. The total splitting of the ground multiplet due to the Gd(III)–Gd(III) interaction is then equal to  $0.42 \text{ cm}^{-1}$ . The EPR spectrum of 2, in contrast with that of 1, is badly resolved; most probably, it corresponds to the envelop of the transitions within all the low-lying states.

Our findings confirm that the intermolecular interaction between two 4f ions can be detected. This interaction, however,

(8) Wasserman, E.; Snyder, L. C.; Yager, W. A. *J. Chem. Phys.* **1964**, *41*, 1763.

is much smaller than that between 3d metal ions, or even between 4f and 3d ions.<sup>9,10</sup> This sequence  $4f-4f < 4f-3d < 3d-3d$  is important as far as the mechanism of the interaction phenomenon is concerned. The molecules  $[\text{Ln}_2(\text{CH}_3\text{CO}_2)_6(\text{phen})_2]$  may be considered as good models to investigate the interaction within pairs of lanthanide(III) ions in a thorough manner. We are presently exploring the consequences of this interaction on the magnetic and optical properties of all the compounds of the series.

### Experimental Section

**Syntheses.** **1** was synthesized as follows:  $\text{Ce}(\text{NO}_3)_3 \cdot 7\text{H}_2\text{O}$  (0.34 g, 0.75 mmol) and  $\text{CH}_3\text{CO}_2\text{Na} \cdot 3\text{H}_2\text{O}$  (0.31 g, 2.28 mmol) were dissolved in 20 mL of methanol. The resulting solution was stirred while a solution of  $\text{phen} \cdot \text{H}_2\text{O}$  (0.15 g, 0.76 mmol) in 20 mL of methanol was added, resulting in a yellow solution. The mixture was stored at room temperature, and compound **1** was collected by filtration as a polycrystalline powder, washed with ethanol, and dried in vacuo. Anal. Calcd for  $\text{C}_{36}\text{H}_{34}\text{N}_4\text{O}_{12}\text{Ce}_2$  (**1**): C, 43.46; H, 3.44; N, 5.63; Ce, 28.17. Found: C, 44.00; H, 3.49; N, 5.63; Ce, 27.60. Single crystals of **1** suitable for crystallographic work were grown by careful layering of 15 mL of a methanolic solution containing 0.042 g of  $\text{Ce}(\text{NO}_3)_3 \cdot 7\text{H}_2\text{O}$ , 0.040 g of  $\text{CH}_3\text{CO}_2\text{Na} \cdot 3\text{H}_2\text{O}$ , and 0.019 g of  $\text{phen} \cdot \text{H}_2\text{O}$  with *n*-hexane

(9) Benelli, C.; Dei, A.; Gatteschi, D.; Pardi, L. *Inorg. Chem.* **1988**, *27*, 2831.

(10) Andruh, M.; Ramade, I.; Codjovi, E.; Guillou, O.; Kahn, O.; Trombe, J. C.; *J. Am. Chem. Soc.* **1993**, *115*, 1822.

at room temperature. The same procedures, using  $\text{Gd}(\text{NO}_3)_3 \cdot 6\text{H}_2\text{O}$  instead of  $\text{Ce}(\text{NO}_3)_3 \cdot 7\text{H}_2\text{O}$  afforded a microcrystalline powder and single crystals of **2**. Anal. Calcd for  $\text{C}_{36}\text{H}_{34}\text{N}_4\text{O}_{12}\text{Gd}_2$  (**2**): C, 42.02; H, 3.33; N, 5.44. Found: C, 41.76; H, 3.42; N, 5.53. X-ray powder patterns revealed that the two compounds, **1** and **2**, were isostructural.

### Crystallographic Data Collection and Structure Determination.

A selected crystal of compound **1** was set up on a Syntex P2<sub>1</sub> automatic diffractometer upgraded by Crystal Logic using Zr-filtered Mo radiation. The structure was solved and refined using SHELX76.<sup>11</sup> Hydrogen atoms were located from a difference map, and refined isotropically. All the other atoms were refined anisotropically. The main crystallographic data are summarized in Table 1. The atomic coordinates of the non-hydrogen atoms are listed in Table 2.

**Acknowledgment.** E.B. acknowledges the Greek Ministry of Industry, Energy, and Technology, General Secretariat of Research and Technology, for financial support (Work No. 1495). A.T. thanks John Boutaris and Sons Co. for financial support.

**Supporting Information Available:** Tables SI–SIV listing the detailed crystallographic data, anisotropic thermal parameters for the non-hydrogen atoms, atomic coordinates and isotropic thermal parameters for the hydrogen atoms, and bond lengths and angles for compound **1** (4 pages). Ordering information is given on any current masthead page.

IC9502887

(11) Sheldrick, G. M. SHELX 76, Programs for Crystal Structure Determinations. University of Cambridge, 1976.